**PHYSICS AND CHEMISTRY OF SOLID STATE**
V. 25, No. 4 (2024) pp. 816-824
*Section: Technology*

**DOI: 10.15330/pcss.25.4.816-824**

*Vasyl Stefanyk Precarpathian National University*

**ФІЗИКА І ХІМІЯ ТВЕРДОГО ТІЛА**
**Т. 25, № 4 (2024) С. 816-824**
*Технічні науки*

PACS: 81.05.Mh

ISSN 1729-4428 (Print)
ISSN 2309-8589 (Online)

Nadiia Hablovska[1], Tetiana Pavlenko[1], Anna Kloc-Ptaszna[2], Łukasz Krzemiński[2], Grzegorz Matula[2],Dariusz Łukowiec[2], Maryna Kononenko[1], Bohdan Hablovskyi[1]

# Synthesis of components for composite material of electrical contacts with unique properties for high-current electrical apparatus with arc-free switching

[1]*Ivano-Frankivsk National Technical University of Oil and Gas, Ivano-Frankivsk, Ukraine, nadiia.hablovska@nung.edu.ua*
[2]*Silesian University of Technology, Poland, Anna.Kloc-Ptaszna@polsl.pl*

Experimental research has determined the optimal composition of components for a composite material used in electrical contacts with unique properties designed for high-current electrical apparatus that perform switching without arc formation. This article presents the results of a study on the porosity of copper obtained by the powder metallurgy method. To analyze the porosity of copper, methods for studying porous structures on both the surface and within the sample were examined. The metallographic method and the method of computed tomography were selected as the most suitable and informative. The conducted studies of the porous material revealed differences in material structure and porosity depending on various manufacturing conditions: temperature, process duration, and ingredient proportions. This, in turn, allowed for the identification of technological parameters for obtaining porous copper with up to 65% porosity, enabling its use as a matrix of the conductive material with a higher melting temperature. The optimal method for infiltrating copper samples with a low-melting material (fusible component) was selected.

**Keywords:** high-current apparatus, electrical contacts, arc-free switching, composite material, porosity, metallographic analysis, computer tomography, infiltration.

*Received 10 June 2024; Accepted 19 November 2024.*

## Introduction

Traditionally, silver has been the primary component for electrical contacts, but recent studies focus on finding alternative, cost-effective materials that provide better electrodynamic stability and lower switching losses [1,2]. A comparison of various materials indicates that composite materials based on powder metallurgy can be used as contact materials with significant advantages due to their unique properties [3,4].

Contacts produced by powder metallurgy methods demonstrate high strength characteristics and improved electro-contact properties [5,6]. This has allowed them to be utilized in the manufacturing of electrical contacts for high-current electrical devices [7]. Composite contacts enable reliable switching without arc formation, which is critical for modern high-performance circuit breakers [2,8].

High-current circuit breakers perform the functions of power distribution in the energy system and provide protection in the event of a malfunction. Therefore, they are essential elements in power engineering. The contact system of high-current circuit breakers includes arc and main contacts, which ensure staged disconnection of the electrical circuit. The main contacts allow for the flow of nominal currents, short-circuit currents within the selective tripping zone, and overload currents. Arc contacts absorb the entire load current when the contacts open, enabling arc switching with the main contacts [10,11].

The key parameters of an automatic circuit breaker are electrodynamic stability, switching capacity, and maximum switching capacity, which influence the mass

and dimensions of the breaker itself. An analysis of the design of automatic circuit breakers has shown that these parameters, which are largely interdependent, are primarily achieved through design solutions – such as separating the contacts into arc and main contacts, further dividing the main contacts into parallel groups, and ensuring the appropriate power consumption of the switching mechanism [12].

The application of sequentially switched main and arc contacts allows for the use of materials for the main contacts that are more resistant to arcing and have low electrical resistance. Typically, such materials exhibit high electrical and thermal conductivity but low hardness. This reduces the required contact pressure to achieve high electrodynamic stability and reduces material costs [13,14]. At the same time, this contact system imposes certain constraints on the overall design and the materials used for manufacturing contacts [6].

Dividing the main contacts into parallel rows within one pole reduces the required total contact pressures while maintaining switching current values and electrodynamic stability. In AC circuit breakers, due to the current displacement effect and the proximity effect, currents through parallel contacts are distributed unevenly - current through the outer contacts is 1.4 - 1.6 times higher than through the middle ones. This naturally leads to a decrease in electrodynamic stability [15].

Electrodynamic stability is further reduced by variations in transition contact resistances, which increase the uneven distribution of current values. This necessitates an increase in active and inductive resistances and a reduction in mutual inductance, which contradicts the main objective - to ensure current flow with minimal losses while reducing the dimensions of the contact system [16].

To enhance the efficiency of contacts and the circuit breaker as a whole, it is essential to strive to reduce the contact resistance in the contact zone and increase electrodynamic stability. Failure to meet these conditions can lead to incomplete contact closure and the occurrence of emergency situations [2,8].

For the reliable operation of electrical devices, the composite material of modern contacts contains expensive, scarce, and toxic elements and compounds. The most common of these include palladium, platinum, silver, copper, nickel, tungsten, cadmium oxide, mercury, and others [1,17].

The need to reduce the content of toxic and expensive components in the composite materials of electrical contacts, as well as to reduce the overall size of devices, makes it relevant to improve, develop, and create a composite material for electrical contacts with special properties for high-current electrical devices with arc-free switching [3,18].

The uniqueness of the proposed composite material lies in the creation of a porous matrix made of a high-melting material impregnated with a filler with a low melting temperature. Under the action of Joule heat, the filler transitions first to a semi-liquid and then to a liquid state, which activates the electrical contacts like liquid-metal ones [7,19]. Electrical contact composites manufactured using this special technology are virtually free of expensive and toxic elements, have low transmission resistance in the contact zone, and high switching capacity. Due to the ability to change the aggregate state of such a composite material and adjust the low-melting component, it is possible to achieve desired property changes within a specified range [21].

Thus, conducting research on porous copper material as a matrix for the low-melting component, selecting the optimal composition and proportions of components when creating porous copper depending on various sample preparation conditions, including temperature and process duration, is an important task [22].

# I. Experiment

### 1.1. Investigated Samples

The samples were prepared using the traditional powder metallurgy technique – by pressing and sintering the powdered material (Fig. 1).

Copper powder from Sigma-Aldrich was used as the primary material, with its characteristics shown in Table 1, along with a pore-forming powder from Sigma-Aldrich.

At the initial stage of sample preparation, a pore-forming powder from Sigma-Aldrich was added to the copper powder. The pore-forming powder was mixed with the copper powders to act as a binder and to create specific levels of porosity in the material. The amounts of pore former and base material were selected experimentally.

The powder mixture was pressed under varying pressures from 1 to 5 tons, with increments of 0.5 tons. The pressure range was determined through preliminary experimental studies [23].

The samples were sintered in a hydrogen atmosphere to prevent oxidation and contamination. The hydrogen flow rate was maintained at a constant 500 cm³/min with a supply pressure of 1 bar during sintering. Sintering was conducted for one hour at three different sintering temperatures: 800°C, 850°C, and 900°C [24]. The sample heating rate was set at 5°C/min, and cooling was performed in the furnace. Sintering at these elevated temperatures caused the pore-forming agent to evaporate from the samples, promoting the formation of pores.

### 1.2. Methodology for Determining Physical Properties of Samples

The study of the physical properties of the obtained samples was conducted in several stages:

- assessment of density characteristics;
- investigation of Vickers microhardness;
- determination of porosity.

The density characteristics of the samples were assessed using the densitometric method [25] with Radwag Type AS310/X laboratory analytical scales (accuracy ±0.1 mg). Density values were calculated according to Equation 1. To improve accuracy, each density calculation was based on three weighings of samples in the respective media.

$$\rho_c = \frac{m_p}{m_p - m_c}\left(\rho_w - \rho_p\right) + \rho_p \qquad (1)$$

where: $\rho_c$ - density of the sample [g/cm$^3$]; $m_p$ - mass of sample measured in air [g]; $m_c$ - mass of sample measured

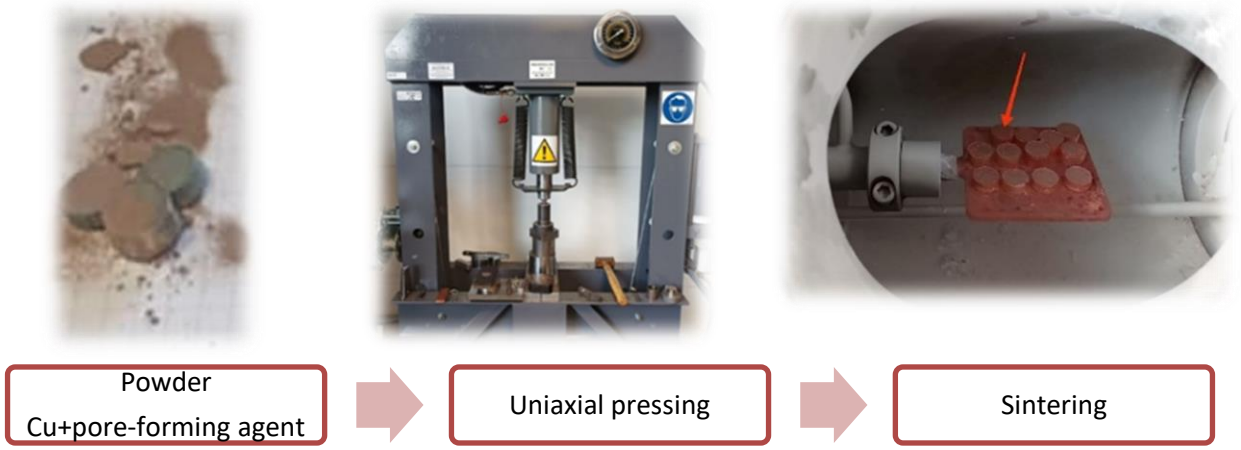


**Fig. 1.** Main Stages of Sample Preparation.

**Table 1.**

Physical Properties of Copper Powder

| Powder | Particle Size ($\mu m$) | Purity (%) | Melting/Boiling Point (°C) | Density (g/cm$^3$) |
|---|---|---|---|---|
| Cu | ≤200 | 99.8 | 1083/2597 | 8.96 |

in water [g]; $\rho_w$ – 0.998203 g/cm$^3$ density of water at T=20±1°C; $\rho_p$ – 0.001205 g/cm$^3$ density of air at T=20±1°C.

For the Vickers microhardness measurements, an FM-ARS 9000 microhardness tester was used with an indenter load of 10 gf and a load duration of 15 seconds [13, 17]. Measurements were conducted on pre-prepared cross-sections of the samples. Overall, microhardness values were determined on 20 randomly selected areas across 5 sections [26].

The final stage of determining the physical properties involved:

- theoretical calculations of the total porosity of the samples using Equation (2) [5]:

$$P = 1 - \frac{\rho_c}{\rho} \cdot 100\%, \qquad (2)$$

where $\rho$ - density without pores [g/cm$^3$].

- tomographic studies using the Nikon ST H 225ST 2X tomograph;

- laboratory stereological studies using a ZEISS Axio Imager [16] optical microscope and AxioVision image analysis software, allowing for the analysis of porous structures within a pore size range that is inaccessible to other methods.

For the tomographic studies, the sample was required to be dry and carefully cleaned of dust. The size and shape of the sample had to be selected to ensure it fit freely in the tomograph chamber and remained stationary during scanning. Failure to meet these requirements could lead to artifacts and "blurred" imaging.

The series of 2D X-ray images obtained from the tomograph was used to reconstruct a three-dimensional model and conduct a detailed analysis of density, shape, geometric characteristics of pores, structural defects, and other physical properties of the sample [6,25].

The images obtained from the microscope and analysis system were used for stereological analysis of the sample structure, assessment of pore distribution, their shape, and geometric characteristics, as well as identification of structural defects and determination of other physical properties of the material [15].

## II. Results and Discussion

To determine the optimal component ratio for creating the desired artificial porosity in the copper sample, experiments were conducted by adding pore-forming agents to copper in a range from 10% to 35% by weight. Analysis of the resulting structures showed that a composition of 75% Cu and 25% pore former achieved an optimal pore distribution, with relatively uniform pore size and placement. The samples were subjected to pressing followed by sintering to evaporate (remove) the pore former, after which porosity analysis was conducted using computed tomography and microscopy.

Before sintering, the sample density varies depending on the applied pressing pressure. At low pressures (1-2.5 t/cm²), the density is lower, while at 3-5 t/cm², it increases, reaching maximum values. After sintering, the density in all samples decreases, indicating an increase in material porosity as a result of pore former removal. This decrease is expected, as pores are formed during sintering, which reduces the overall density.

Samples pressed at 3-5 t/cm² show the most stable density values both before and after sintering, indicating that this pressure range is optimal for ensuring material structural stability. At pressures of 1-2.5 t/cm², the post-sintering density exhibits greater variation, suggesting insufficient or excessive compactness. Samples pressed at 3-5 t/cm² achieve higher densities before sintering than samples pressed at lower pressures, confirming the suitability of this pressure range for achieving high density. After sintering, samples pressed at 3-5 t/cm² show a stable and predictable reduction in density, making this parameter suitable for achieving reproducible results.

Thus, density studies indicate that a pressure range of 3 to 5 t/cm² provides the best balance between compactness before sintering and stability after sintering.

This makes it optimal for creating a porous structure with predictable density characteristics, which is important for the material's subsequent use in composites.

Vickers hardness values confirm that higher pre-sintering density correlates with higher microhardness. Samples with high initial density exhibit greater strength and lower porosity, which generally enhances the microhardness of the resulting structures. When pre-sintering density ranges from 4.5 to 5.0 g/cm³, microhardness reaches maximum levels of around 160–170 HV. In contrast, samples with lower pre-sintering density, between 3.5 and 4.0 g/cm³, have hardness values around 90–100 HV, highlighting the importance of selecting an optimal density to achieve the desired mechanical properties.

After sintering, all samples exhibit a reduction in density, indicating an increase in material porosity. This is expected, as the removal of the pore-forming agent leads to pore formation in the structure. Post-sintering microhardness values show that samples with higher porosity tend to have lower hardness values. In samples with high porosity, hardness decreases to 110-120 HV, while less porous samples demonstrate hardness values in the range of 140-150 HV.

Pressing at pressures of 3 to 5 t/cm² provides more stable density values both before and after sintering, allowing for a uniform distribution of microhardness. Samples produced within this pressure range demonstrate reliable mechanical properties and relatively stable microhardness values both before and after sintering. This makes this pressure range optimal for applications where stable strength and result reproducibility are essential.

The porosity analysis of the copper samples conducted using computed tomography provided important insights into the pore structure. The total pore volume in the sample is approximately 52.36 mm³. The average pore volume is 0.00328 mm³ [5,25], indicating the presence of both small and large pores [12,13]. It illustrates the frequency of pores of different volumes, highlighting the predominance of small pores and a minor presence of large pores (Fig. 2).

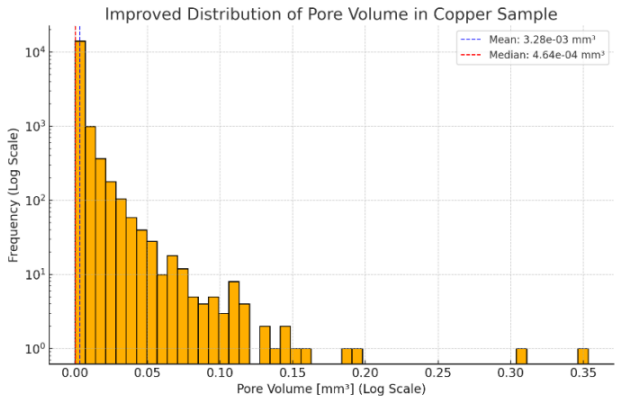


**Fig. 2.** Histogram of Pore Volume Distribution in the Copper Sample.

A logarithmic scale was used to construct the graph, allowing for better representation of both large and small pores [6,14]. Added lines for mean and median values (blue and red lines, respectively) help visually assess the main statistical distribution characteristics.

The pores exhibit an irregular shape, as evidenced by an average sphericity of 0.528 and a compactness of 0.278. These values indicate a deviation from the ideal spherical shape, especially for larger pores, which tend to be more elongated [2].

The compactness distribution (Fig. 3) reflects the variety of pore shapes, ranging from more elongated to compact forms, with most values located in the lower part of the scale, indicating the presence of elongated shapes [3,19].

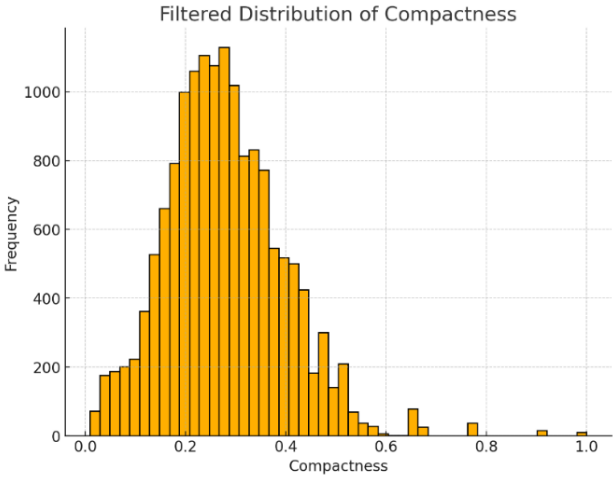


**Fig. 3.** Compactness Distribution.

The sphericity distribution (Fig. 4) shows that most pores have a sphericity value below 1, indicating that the pores are predominantly irregular, with a slight tendency toward rounded forms.

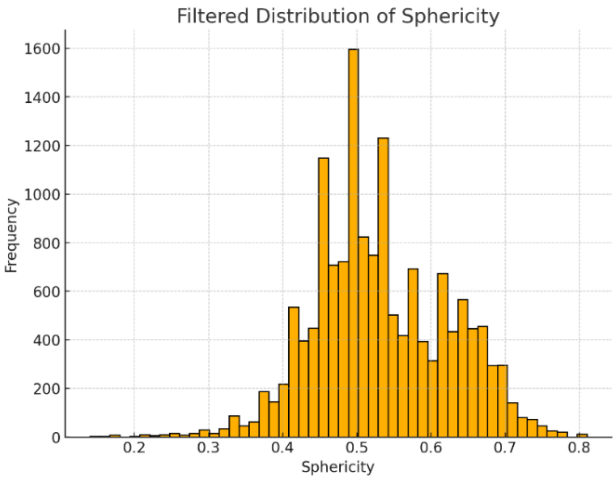


**Fig. 4.** Sphericity Distribution.

Most pores have sphericity values ranging from 0.47 to 0.59, which reflects a predominantly irregular shape. A weak inverse relationship between pore volume and sphericity was also identified, suggesting that larger pores tend to have lower sphericity and a more elongated form [15].

Computed tomography enabled the three-dimensional reconstruction of the sample, allowing for an assessment of the spatial distribution of pores. The projected areas and dimensions along the x, y, and z axes demonstrated variability in shapes within the 3D space, with an average

pore size of 0.158 mm along the x-axis, 0.132 mm along the y-axis, and 0.139 mm along the z-axis [26].

Fig. 5 presents a three-dimensional analysis of the porosity of the copper sample, performed using computed tomography. The colored pores in the upper images are identified by size, with larger pores marked in red and smaller ones in blue and green [16,18]. This visual representation allows for an assessment of the variability in pore sizes and shapes. The lower right image shows a 3D reconstruction of the sample's porous structure, enabling the examination of pore distribution in space and the evaluation of the spatial relationships among cavities.

The analysis of the correlation matrix (Fig. 6) of pore characteristics in the porous copper sample indicates that pore volume has a strong positive correlation with characteristics such as equivalent diameter, surface area, and voxel count [2,27]. This suggests that larger pores generally have a greater diameter, surface area, and voxel count, which logically corresponds to their larger volume. Equivalent diameter also has a high correlation with surface area, indicating a direct relationship between pore size and its surface area.

Sphericity shows weak correlations with most other parameters, except for compactness, with which it exhibits a moderate negative correlation [20]. This implies that more spherical pores are less elongated or compact,

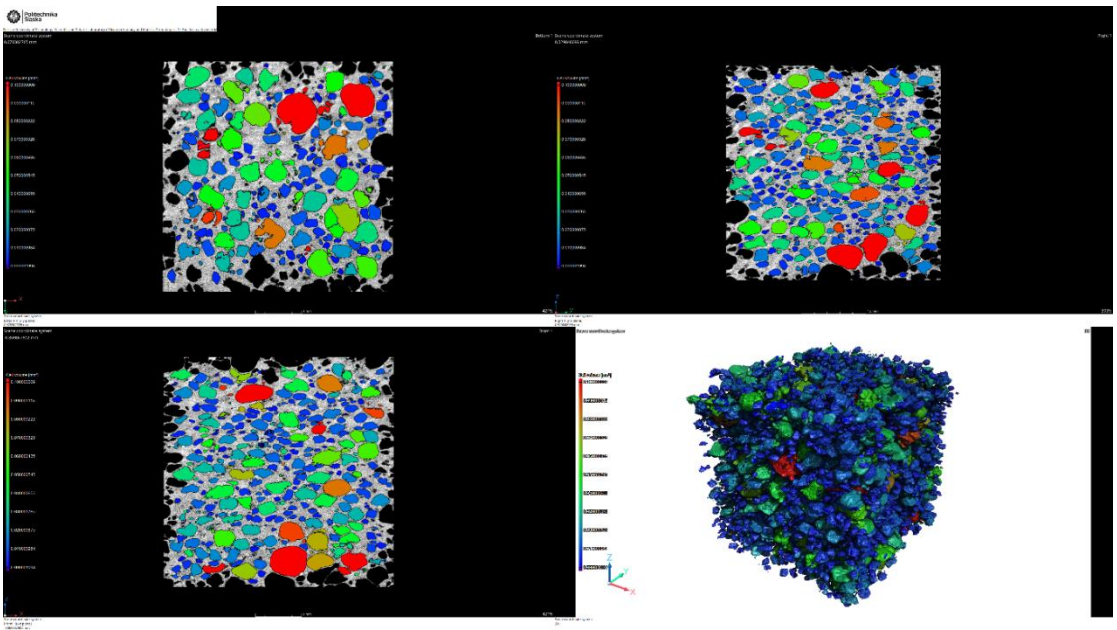

**Fig. 5.** Three-Dimensional Reconstruction of the Porous Structure of the Copper Sample Based on Computed Tomography Results.

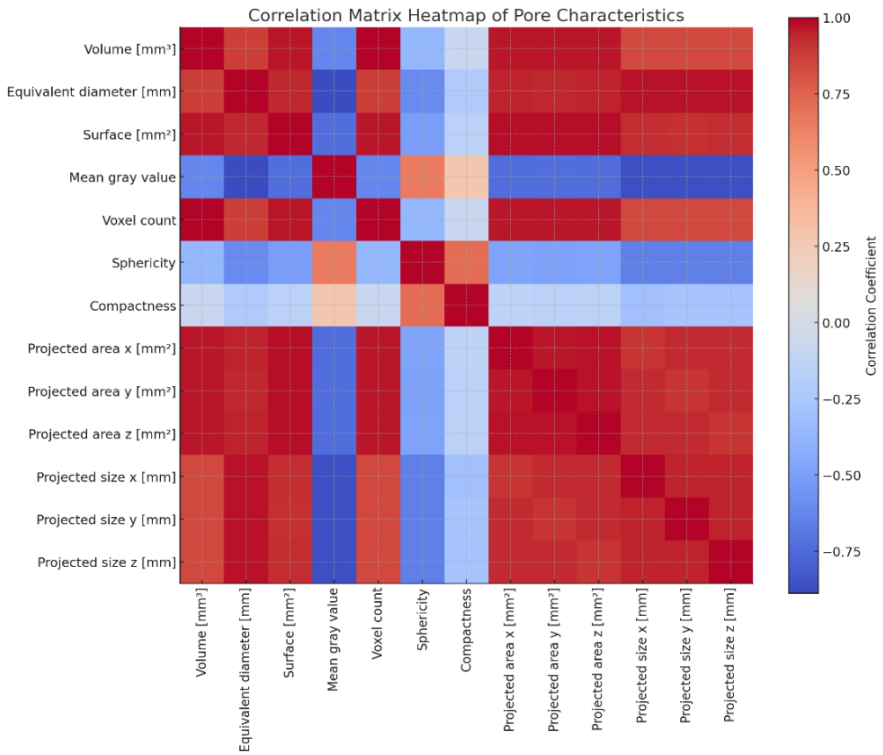


**Fig. 6.** Correlation Matrix of Pore Characteristics in the Porous Copper Sample.

supporting their tendency toward a rounder shape. Compactness, in turn, shows a weak inverse relationship with volume and surface area, suggesting that elongated pore shapes have smaller volumes or surface areas. The projected areas and dimensions along the x, y, and z axes exhibit moderate correlations with volume, equivalent diameter, and surface area [28]. This suggests that the three-dimensional shape of pores partially determines their volume and size.

Thus, the correlation matrix demonstrates that the size and shape of pores in the porous copper sample are not random values but are interconnected through specific geometric characteristics [6,19]. This confirms that larger pores tend to have a greater surface area and volume, as well as a more elongated shape, while pores with high sphericity are more rounded.

The graph (Fig. 7) shows the relationship between pore compactness and sphericity in the sample. Overall, an inverse trend can be observed: pores with higher compactness exhibit lower sphericity, indicating a more elongated or irregular shape [26]. Pores with high sphericity tend to approximate a spherical form but usually have lower compactness values, suggesting their rounded nature.

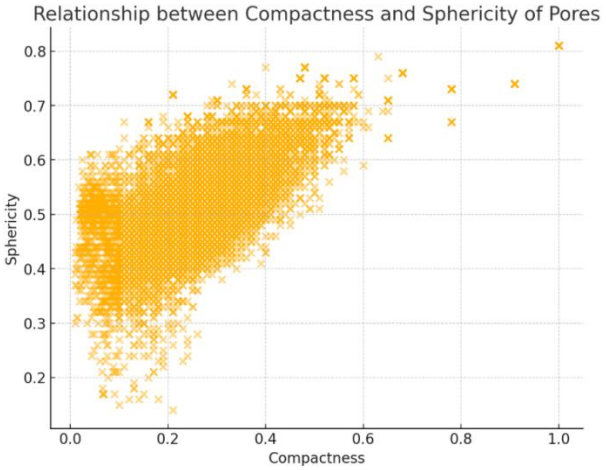


**Fig. 7.** Relationship between Compactness and Sphericity of Pores.

This analysis confirms that compactness and sphericity metrics complement each other in evaluating pore shape, where more spherical pores are less compact, and more elongated pores are more compact.

The study of copper sample microsections under a microscope complements the results of computed tomography, providing detailed images of pore structure at the surface level [15,27]. In the micrograph (Fig. 8), pores of various sizes and shapes are evenly distributed across the matrix. Dark areas represent pores, while light regions correspond to the copper matrix.

It can be seen that larger pores have irregular shapes, while smaller ones tend to be closer to spherical. This pore morphology supports the tomography results, which also indicated an irregular shape for larger pores and a predominance of smaller, rounded pores.

The micrograph shows a uniform distribution of pores of various shapes and sizes within the copper matrix, confirming the presence of significant porosity [4,16].

Combining the microscopy and computed tomography results provides a comprehensive view of the porous sample structure. Computed tomography offers a three-dimensional perspective on porosity, illustrating the distribution of pore volume and shape throughout the sample [18]. Meanwhile, micrographs of microsections provide highly detailed images of pores at the surface level, allowing for an assessment of pore morphological features, such as edges and geometry.

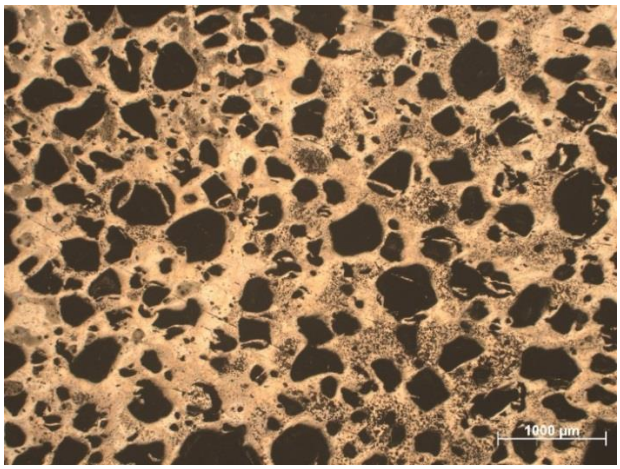


**Fig. 8.** Microstructure of the Porous Copper Sample.

It can be observed that the pore structure within the copper matrix is relatively homogeneous throughout the sample and contains numerous pores with irregular shapes. This is an important characteristic for the use of such materials in composites, as high porosity and a variety of pore shapes facilitate further infiltration with materials of low melting points.

## Conclusions

The study of the porous structure of copper samples, produced using powder metallurgy, provided a detailed characterization of the material, which can be utilized as a matrix for electrical contacts in high-current electrical devices. By employing computed tomography and microstructural analysis of microsections, the unique features of the porous structure of the samples were revealed at both the surface and volumetric levels.

Computed tomography enabled an assessment of the total pore volume in the sample, which is 52.36 mm³. It was also determined that the average pore volume is 0.00328 mm³, and the pore shapes are predominantly irregular, with an average sphericity of 0.528. This indicates a predominance of elongated and uneven shapes, especially for larger pores, which was further confirmed by the compactness and sphericity distributions.

A comparative analysis of computed tomography and micrograph results showed that the porous structure of the copper matrix is homogeneous and contains numerous pores of various shapes and sizes. The micrographs confirmed that larger pores exhibit irregular shapes, while smaller pores are closer to spherical, which aligns with the 3D tomography data.

The results enabled the establishment of optimal technological parameters for producing porous copper with the required porosity. Such a structure shows

potential as a matrix for a low-melting component, which can significantly improve thermal conductivity, reduce electrical resistance in the contact zone, and increase the electrodynamic stability of the contact system.

The developed material and its production technology offer an economically viable alternative to traditional contact materials by enabling the replacement of costly and scarce elements, such as silver and platinum. A composite based on porous copper, impregnated with a low-melting material, has the potential for use in high-current circuit breakers and other electrical devices where low transition resistance, high thermal conductivity, and efficient arc-free switching are essential.

Thus, the combination of computed tomography and microstructural analysis of microsections has allowed for a detailed examination of the structure and properties of the porous copper material, which is a crucial step in developing innovative materials for electrical engineering applications.

***Hablovska Nadiia –*** PhD of Technical Science, Associate Professor of the Electrical Power Engineering Department, Ivano-Frankivsk National Technical University of Oil and Gas;
***Pavlenko Tetiana*** - Doctor of Technical Science, Professor of the Electrical Power Engineering Department Ivano-Frankivsk National Technical University of Oil and Gas;
***Kloc-Ptaszna Anna*** – PhD, Department of Engineering and Biomedical Materials, Faculty of Mechanical Engineering, Silesian University of Technology;
***Krzemiński Łukasz*** – PhD, Scientific and Teaching Laboratory of Nanotechnology and Material Technologies – RMT-L2, Faculty of Mechanical Engineering, Silesian University of Technology;
***Matula Grzegorz –*** Professor, Scientific and Educational Laboratory of Nanotechnology and Material Technologies, Faculty of Mechanical Engineering, Silesian University of Technology;
***Łukowiec Dariusz –*** PhD, Materials Research Laboratory, Faculty of Mechanical Engineering, Silesian University of Technology;
***Kononenko Maryna*** - PhD of Technical Science, Associate Professor of the Metrology and Information-measuring Technology Department Ivano-Frankivsk National Technical University of Oil and Gas;
***Hablovskyi Bohdan*** – PhD of Geological Sciences, Associate Professor of the Department of Oil and Gas Geophysics Ivano-Frankivsk National Technical University of Oil and Gas.

[1] A. Chen, B. Li, C. Zhang, *Innovative design of porous materials for advanced thermal management*, Sustainable Materials and Technologies, 36, 110562 (2024); https://doi.org/10.1016/j.mtcomm.2024.110562.
[2] S.Y. Tarasov, A.A. Kudryavtsev, *Microstructure and Properties of Composite Materials in High-Current Electrical Contacts*, Materials Today: Proceedings, 4(3), 2820 (2017); https://doi.org/10.1016/j.matpr.2017.02.160.
[3] Y. Cao, X. Jiang, *Powder Metallurgy Processing of Copper and Copper-Based Materials*, Materials Science Forum, 959, 17 (2019); https://doi.org/10.4028/www.scientific.net/MSF.959.17.
[4] F. Wan, T.J. Pirzada, R. Liu, Y. Wang, C. Zhang, & T.J. Marrow, *Microstructure Characterization by X-Ray Computed Tomograp hy of C/C-SiC Ceramic Composites Fabricated with Different Carbon Fiber Architectures*, Applied Composite Materials, 26, 1247; https://doi.org/10.1007/s10443-019-09778-2.
[5] T.M. Mazur, M.M. Slyotov, M.P. Mazur, V.V. Prokopiv, O.I. Kinzerska, O.M. Slyotov, *Features of the cadmium chalcogenide substrates with surface nanostructure*, Materials Today: Proceedings, 35 (4), 661 (2019); https://doi.org/10.1016/j.matpr.2019.12.112.
[6] S. Khademzadeh, S. Carmignato, N. Parvin, F. Zanini, P. F. *Bariani, Micro porosity analysis in additive manufactured NiTi parts using micro computed tomography and electron microscopy*, Materials and Design, 90, 745 (2016); https://doi.org/10.1016/j.matdes.2015.10.161.
[7] M.M. Slyotov, T.M. Mazur, V.V. Prokopiv, O.M. Slyotov, M.P. Mazur, *Sources of optical radiation based on ZnTe/ZnSe/ZnS heterostructures*, Materials Today: Proceedings, 62, 5763, (2022); https://doi.org/10.1016/j.matpr.2022.03.476.
[8] S. Hong, J. Kim, *The Role of Sintering Additives in the Sintering of Copper and Its Alloys*, Acta Materialia, 54(2), 301 (2006); https://doi.org/10.1016/j.actamat.2005.09.015.
[9] R. Cavuoto, P. Lenarda, A. Tampieri, D. Bigoni, & M. Paggi, *Phase-field modelling of failure in ceramics with multiscale porosity*. Materials & Design, 238, 112708 (2024); https://doi.org/10.1016/j.matdes.2024.112708.
[10] J. Čapek, D. Vojtěch, *Properties of porous magnesium prepared by powder metallurgy*, Materials Science and Engineering C, 33(1), 564 (2013); https://doi.org/10.1016/j.msec.2012.10.002.
[11] N.T. Aboulkhair, N.M. Everitt, I. Ashcroft, C. Tuck, *Reducing porosity in AlSi10Mg parts processed by selective laser melting*, Additive Manufacturing, 1(4), 77 (2014); https://doi.org/10.1016/j.addma.2014.08.001.
[12] M. Elangovan, S. Gowri, N. Velmurugan, *Investigating the morphology, hardness, and porosity of copper filters produced via hydraulic pressing*, Journal of Materials Research and Technology, 19, 208 (2022); https://doi.org/10.1016/j.jmrt.2022.05.012.
[13] T.M. Mazur, V.V. Prokopiv, M.M. Slyotov, M.P. Mazur, O.V. Kinzerska, O.M Slyotov, *Optical properties of CdTe doped Ca*, Physics and chemistry of solid state, 21(1), 52 (2020); https://doi.org/10.15330/pcss.21.1.52-56.
[14] V. S. Seesala, R. Rajasekaran, A. Dutta, P. V. Vaidya, S. Dhara, *Dense-porous multilayer ceramics by green shaping and salt leaching*, Open Ceramics, 5, 100084 (2021); https://doi.org/10.1016/j.oceram.2021.100084.

[15] A. Hedayati, M. Heshmati, H. Faghih Shojaei, M. Salimi, *Optimization of porosity and permeability in metal foams using a combined experimental and numerical approach*, Powder Technology, 392, 229 (2021); https://doi.org/10.1016/j.powtec.2021.06.009.

[16] E.M. Kiass, K. Zarbane, Z. Beidouri, *Process parameters effect on porosity rate of AlSi10Mg parts additively manufactured by Selective Laser Melting: challenges and research opportunities*, Archives of Materials Science and Engineering, 122(1), 22 (2023); https://doi.org/10.5604/01.3001.0053.8844.

[17] A.Y. Al-Maharma, S.P. Patil, B. Markert, *Effects of porosity on the mechanical properties of additively manufactured components: a critical review*, Materials Research Express, 7, 122001 (2020); https://doi.org/10.1088/2053-1591/abcc5d.

[18] W. Sun, S. B. Brown, R. K. Leach, *An overview of industrial X-ray computed tomography, NPL Report ENG 32*, National Physical Laboratory, January (2012).

[19] A. J. Kinloch, R. J. Young, *Fracture Behavior of Polymers*, Applied Science Publishers, 1983.

[20] Z. Fan, B. Zhang, Y. Liu, T. Suo, P. Xu, J. Zhang, *Interpenetrating phase composite foam based on porous aluminum skeleton for high energy absorption*, Polymer Testing, 93, 106917 (2021); https://doi.org/10.1016/j.polymertesting.2020.106917.

[21] C. Hall, *Concrete Microstructure*, Properties, and Materials, McGraw-Hill Education, 1994.

[22] M. Sinico, S. D. Jadhav, A. Witvrouw, K. Vanmeensel, W. Dewulf, *A Micro-Computed Tomography Comparison of the Porosity in Additively Fabricated CuCr1 Alloy Parts Using Virgin and Surface-Modified Powders*, Materials, 14(8), 1995 (2021); https://doi.org/10.3390/ma14081995.

[23] Pavlenko, T., Hablovska, N., & Shyndak, L. *Analysis of the possibility of using pseudo-liquid metal contacts in electrical devices.* International Science Journal of Engineering & Agriculture, 2(2), 64 (2023); https://doi.org/10.46299/j.isjea.20230202.06.

[24] N. Hablovska, T. Pavlenko, G. Matula, D. Lukowiec, A. Kloc-Ptaszna, Ł. Krzemiński, *Studies on the porosity of copper used as a matrix for conductive composite for high-current circuit breakers with arc-free switching*, Perspectives of Development in Engineering Sciences – Trends, Innovations and Challenges, Vol. 2, TYGIEL Scientific Publishing House, Lublin, 74 (2024); https://bc.wydawnictwo-tygiel.pl/publikacja/35E7EC54-B2A8-0E00-DFBE-3F20777FE701

[25] A.N.S. Appiah, A. Woźniak, P. Snopiński, K. Matus, P.M. Nuckowski, G.F. Batalha, S.A. Nazarov, I.N. Ganiev, M. Adamiak, *Vanadium-induced structural effects on the corrosion and tribological properties of an Al-Li binary alloy*, Journal of Alloys and Compounds, 973, 172910 (2024); https://doi.org/10.1016/j.jallcom.2023.172910.

[26] C. Kamath, B. El-Dasher, G.F. Gallegos, W.E. King, A. Sisto, *Density of additively-manufactured, 316L SS parts using laser powder-bed fusion at powers up to 400 W*, International Journal of Advanced Manufacturing Technology, 74, 65 (2014); https://doi.org/10.1007/s00170-014-5954-9.

[27] R. Liu, S. Liu, X. Zhang, *A physics-informed machine learning model for porosity analysis in laser powder bed fusion additive manufacturing*, International Journal of Advanced Manufacturing Technology, 113, 1943 (2021); https://doi.org/10.1007/s00170-021-06640-3.

[28] [C.L. Reedy, C.L. Reedy, *High-resolution micro-CT with 3D image analysis for porosity characterization of historic bricks*, Heritage Science, 10, 83 (2022); https://doi.org/10.1186/s40494-022-00723-4.

Н.Я. Габльовська[1], Т.М. Павленко[1], А. Клоц-Пташна[2], Л. Кжемінскі[2], Г. Матула[2], Д. Луковіч[2], М.А. Кононенко[1], Б.Б. Габльовський[1]

# Синтез компонентів композитного матеріалу електричних контактів з особливими властивостями для високоамперних електричних апаратів з бездуговою комутацією

[1]*Івано-Франківський національний технічний університет нафти і газу, Івано-Франківськ, Україна, nadiia.hablovska@nung.edu.ua*
[2]*Сілезький технологічний університет, Польща, Anna.Kloc-Ptaszna@polsl.pl*

Шляхом проведення експериментальних досліджень встановлено оптимальний склад компонентів для композитного матеріалу, що використовується в електричних контактах, з особливими властивостями, призначених для високострумових електричних апаратів, які здійснюють комутацію без утворення дуги. В даній статті наведено результати дослідження пористості міді, одержаної за методом порошкової металургії. Для проведення аналізу пористості міді було проаналізовано методи дослідження пористих структур, як на поверхні, так і в тілі зразка. Як найбільш придатними і інформативними було обрано металографічний метод та метод комп'ютерної томографії. Проведені дослідження пористого матеріалу дозволили стверджувати про відмінності у структурі матеріалу та пористості в залежності від різних умов виготовлення зразків: температури та тривалості процесів, пропорції інгредієнтів. А це, в свою чергу, дозволило визначити технологічні параметри одержання пористої міді з пористістю до 65%, що уможливлює її використання, як матриці провідного матеріалу – складової з вищою температурою плавлення. Підібрано оптимальний метод інфільтрації мідних зразків матеріалом з низькою температурою плавлення (легкоплавкою складовою).

**Ключові слова:** високострумові апарати, електричні контакти, бездугова комутація, композитний матеріал, пористість, металографічний аналіз, комп'ютерна томографія, інфільтрація.